

longer than the remaining four bonds in the ring, which average 1.377 (5) Å. Accordingly, this distribution of bond lengths suggests that a small contribution to the stability of this anion is made by some S-C multiple bonding (and inductive electron withdrawal), which localizes double-bond character at C(3)-C(4) and also at C(5)-C(6) and C(1)-C(6).

**Acknowledgment.** We thank Dr. Fred Hollander of the Berkeley CHEXRAY Diffraction Facility (supported in part by the National Science Foundation) for assistance and Susan J. Barclay for helpful suggestions during the preparation of

this manuscript. This work was supported in part by the Director, Office of Energy Research, Office of Basic Energy Sciences, Chemical Sciences Division of the U.S. Department of Energy, under Contract No. DE-AC03-76SF00098.

**Registry No.** 1, 86709-65-1; 2, 86709-67-3;  $\text{Ag}_2(\text{C}_6\text{Cl}_2\text{O}_4)$ , 86709-66-2; *o*-chloranil, 2435-53-2.

**Supplementary Material Available:** Listings of anisotropic thermal parameters and observed and calculated structure factor amplitudes (Tables IV-VII) and a stereoscopic view of **2** (Figure 6) (22 pages). Ordering information is given on any current masthead page.

Contribution from the Departments of Chemistry, University of California, Berkeley, California 94720, and University of Vermont, Burlington, Vermont 05405

### Siderophilin Metal Coordination. 3. Crystal Structures of the Cobalt(III), Gallium(III), and Copper(II) Complexes of Ethylenebis(*o*-hydroxyphenyl)glycine<sup>1</sup>

PAUL E. RILEY,<sup>2a</sup> VINCENT L. PECORARO,<sup>2a</sup> CARL J. CARRANO,<sup>2b</sup> and KENNETH N. RAYMOND\*<sup>2a</sup>

Received August 24, 1982

The structures of the Co(III), Ga(III), and Cu(II) complexes of the hexadentate ligand ethylenebis(*o*-hydroxyphenyl)glycine (EHPG) have been determined by single-crystal X-ray diffraction techniques using data collected by counter methods. These complexes are used as models for the metal binding site of the human iron transport protein transferrin. While solutions of the complexed metals were composed of mixtures of racemic and mesomeric ligands, for all three metal complexes the only crystals obtained were those of the racemic isomer of EHPG. Deep red prisms of  $[\text{Co}(\text{H}_2\text{O})_6][\text{Co}(\text{EHPG})]_2 \cdot 4\text{H}_2\text{O}$  (**1**) crystallize in the monoclinic space group  $P2_1/n$  with  $a = 14.818$  (2) Å,  $b = 16.991$  (2) Å,  $c = 8.414$  (1) Å, and  $\beta = 91.32$  (1)°. The calculated density of 1.676 g cm<sup>-3</sup> for  $Z = 2$  compares satisfactorily with the measured value of 1.61 (3) g cm<sup>-3</sup>. Large, irregular, pale orange crystals of  $[\text{Mg}(\text{H}_2\text{O})_6][\text{Ga}(\text{EHPG})]_2 \cdot 3\text{H}_2\text{O}$  (**2**) form in the monoclinic space group  $C2/c$  with  $a = 20.946$  (4) Å,  $b = 13.010$  (1) Å,  $c = 17.002$  (3) Å, and  $\beta = 114.75$  (1)° and are isostructural with  $[\text{Mg}(\text{H}_2\text{O})_6][\text{Fe}(\text{EHPG})]_2 \cdot 3\text{H}_2\text{O}$ , which was reported earlier. The value of the calculated density of 2 of 1.639 g cm<sup>-3</sup> for  $Z = 4$  is in agreement with the measured value of 1.56 (3) g cm<sup>-3</sup>. Deep blue-green prisms of  $\text{Na}_2[\text{Cu}(\text{EHPG})] \cdot 5.5\text{H}_2\text{O}$  (**3**) crystallize in the orthorhombic space group  $Pbcn$  with  $a = 14.195$  (1),  $b = 22.607$  (3), and  $c = 14.242$  (1) Å. The calculated density of 1.641 g cm<sup>-3</sup> for  $Z = 8$  agrees well with the measured density of 1.61 (3) g cm<sup>-3</sup>. In each structure, the metal ion is bound by the two nitrogen atoms, the two phenolate oxygen atoms, and the two carboxylate oxygen atoms, so as to describe a pseudooctahedral geometry about the metal with the carboxylate ligands trans to each other. Each complex displays virtual  $C_2$  symmetry. In contrast, in the previously reported structure of the  $\text{Na}^+$  salt of the meso complex of  $[\text{Fe}(\text{EHPG})]^-$  (which cannot have  $C_2$  symmetry because it possesses both  $R$  and  $S$  centers in the ligand), the three pairs of chemically equivalent donor atoms are mutually cis. Although the structure of **3** suffers from disorder of the  $\text{Na}^+$  ions over several similar coordination environments, the structure of the  $[\text{Cu}(\text{EHPG})]^{2-}$  species is satisfactorily determined and exhibits an anticipated tetragonal elongation (by 0.4–0.5 Å) of the axial Cu–O(carboxylate) bonds. As a consequence of the cation disorder, the resultant  $\text{Na}^+$  content per unit cell, as ascertained by least-squares refinement of  $\text{Na}^+$  occupancy parameters, is 13.9 (2) ions rather than the 16 ions required by stoichiometry. Full-matrix least-squares refinements of the structures have converged with conventional (and weighted)  $R$  indices (on  $|F|$ ) of 0.025 (0.031), 0.033 (0.035), and 0.052 (0.064) for **1**, **2**, and **3**, respectively, using (in the same order) 3536, 3778, and 2508 observations of  $|F_o|$  with  $F_o^2 > 3\sigma(F_o^2)$ .

#### Introduction

The mechanisms of iron exchange, assimilation, transport, and utilization by immature red blood cells are of critical interest in the field of iron metabolism. The subsequent implications of these processes with respect to the treatment of various blood disorders are especially significant. A key component of mammalian iron biochemistry is the serum protein transferrin, which shuttles iron from points of absorption and storage to the reticulocytes for utilization in heme synthesis.<sup>3</sup> Therefore, a thorough understanding of transferrin chemistry is prerequisite to a detailed description of iron metabolism.

Human serum transferrin is a glycoprotein of molecular weight 80 000, which is capable of binding two ferric ions

tightly but reversibly.<sup>4</sup> Although the area of transferrin chemistry has been studied extensively for many years, several important questions still remain unanswered. One of the most important of these is the nature and number of ligating groups that comprise the metal binding sites.

Recently we have begun to gain further insight into these questions by the examination of suitable small-molecule model compounds that mimic the physical properties of the iron binding sites of transferrin.<sup>1,5,6</sup> Presently these models are based on ethylenebis(*o*-hydroxyphenyl)glycine (EHPG) (Figure 1), which incorporates the ligating groups previously implicated in the metal binding sites.<sup>4</sup> On the basis of its optical and resonance Raman spectra,  $\text{Fe}^{\text{III}}\text{EHPG}$  has long been recognized as a potential model for the iron binding site of transferrin.<sup>7,8</sup> One area of our current interest has been

(1) Previous paper in this series: Pecoraro, V. L.; Harris, W. R.; Carrano, C. J.; Raymond, K. N. *Biochemistry* 1981, 20, 7033.

(2) (a) University of California, Berkeley. (b) University of Vermont.

(3) Crichton, R. R., Ed. "Problems of Iron Storage and Transport in Biochemistry and Medicine"; North Holland Publishing Co.: Amsterdam, 1975.

(4) Chasteen, N. D. *Coord. Chem. Rev.* 1977, 22, 1.

(5) Harris, W. R.; Carrano, C. J.; Pecoraro, V. L.; Raymond, K. N. *J. Am. Chem. Soc.* 1981, 103, 2231.

(6) Patch, M. G.; Simolo, K. S.; Carrano, C. J. *Inorg. Chem.* 1982, 21, 2972.

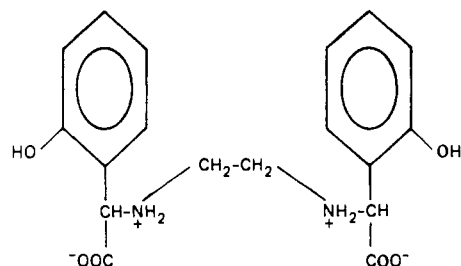


**Figure 1.** Schematic drawing of ethylenebis(*o*-hydroxyphenyl)glycine (EHPG).

to extend this comparison to other physical properties and to metals other than iron.<sup>6</sup> We have investigated in detail the perturbation of the ultraviolet difference spectrum upon coordination of a variety of metals to EHPG and have used these data to reinterpret the analogous transferrin results.<sup>1</sup>

Critical to the use of EHPG as a model is a detailed knowledge of the structures of its metal complexes. Structures of the iron complexes have recently been reported.<sup>9,10</sup> We describe here the crystal structures of the diamagnetic Co(III) and Ga(III) complexes, which may be useful in determining the solution conformation of EHPG metal complexes by NMR and also that of the paramagnetic, tetragonally distorted Cu(II) derivative, which has previously been used to probe the spectral properties of transferrin.<sup>1,7</sup>

### Experimental Section

**Materials.** The ligand (EHPG) was purchased from Sigma Chemicals, purified as previously described,<sup>1</sup> and stored under nitrogen. No attempt was made to separate the racemic and mesomeric isomers of the ligand, which are present in an unspecified mixture in commercial preparations and found to be in approximately 1:1 ratios in our samples. Metallic salts were analytical grade and were used as supplied.

**Microanalyses.** Chemical analyses were performed by the Microanalytical Laboratory, Department of Chemistry, University of California, Berkeley, CA, or by Schwarzkopf Mikroanalytical Laboratories Woodside, NY. Metal concentrations in coordination compounds were determined by atomic absorption spectroscopy, which was also conducted locally.

The vis/UV spectra of the  $[\text{Cu}(\text{EHPG})]^{2-}$  compound were measured in aqueous solution at pH 10 with a Hewlett-Packard 8450 spectrophotometer.

**Syntheses.**  $[\text{Co}(\text{H}_2\text{O})_6][\text{Co}(\text{EHPG})_2] \cdot 4\text{H}_2\text{O}$  (**1**). This complex was prepared via a modification of the procedure of Sugira et al.<sup>11</sup> The EHPG ligand was dissolved by using 2 equiv of NaOH, and then the solution was treated with a stoichiometric amount of cobaltous chloride. The mixture was stirred in air for several days. When necessary, Co(II) was oxidized by the addition of aliquots of  $\text{H}_2\text{O}_2$  until there was no further absorbance increase at  $\sim 520$  nm. The solution was then filtered and flash evaporated. The residue was purified by repeated extractions with hot ethanol. Deep red crystals, suitable for X-ray diffraction, were obtained by slowly cooling a hot aqueous solution and were shown to be of the racemic isomer of EHPG as determined by TLC on silica gel in a butanol/water/acetic mixture [4:1:1 (upper layer)].<sup>6</sup>

Anal. Calcd for  $[\text{Co}(\text{H}_2\text{O})_6][\text{Co}(\text{EHPG})_2] \cdot 4\text{H}_2\text{O}$ : C, 40.4; H, 4.86; N, 5.24. Found: C, 40.3; H, 4.88; N, 5.73.

$[\text{Mg}(\text{H}_2\text{O})_6][\text{Ga}(\text{EHPG})_2] \cdot 3\text{H}_2\text{O}$  (**2**). A stoichiometric amount of an acidic  $\text{Ga}(\text{NO}_3)_3$  solution (pH 1.2) was added to 1.3 mmol of a basic aqueous solution (25 mL) of EHPG. A 2-equiv portion of magnesium was introduced into the solution as the carbonate salt.

The pH of the solution was adjusted to 7.2 with  $\text{HNO}_3$  and then filtered. When the mixture was allowed to stand at room temperature for 2 weeks, large pale orange irregular crystals with a pseudooctahedral habit were obtained.

Anal. Calcd for  $[\text{Mg}(\text{H}_2\text{O})_6][\text{Ga}(\text{EHPG})_2] \cdot 3\text{H}_2\text{O}$ : Ga, 13.2; Mg, 2.3; C, 40.93; H, 4.96; N, 5.31. Found: Ga, 16.6; Mg, 2.20; C, 37.56; H, 4.81; N, 5.63.

$\text{Na}_2[\text{Cu}(\text{EHPG})] \cdot 5.5\text{H}_2\text{O}$  (**3**). Addition of 15 mmol of  $\text{CuCl}_2$  to a basic aqueous solution of EHPG (10 mmol, 50 mL) afforded a deep blue-green solution, which was filtered and treated with aqueous NaOH until the pH was 9.8. Slow evaporation ( $\sim 1$  week) at room temperature yielded dark blue-green prisms. During this time the pH of the solution dropped to 9.1. Analysis of the bulk material corresponds closely to the pure sodium salt of  $[\text{Cu}(\text{EHPG})]^{2-}$ .

Anal. Calcd for  $\text{Na}_2[\text{Cu}(\text{EHPG})] \cdot 5.5\text{H}_2\text{O}$ : C, 38.3; H, 4.82; N, 4.96; Cu, 11.2; Na, 8.14. Found: C, 39.13; H, 4.71; N, 4.70; Cu, 10.2; Na, 8.39.

### X-ray Crystallography

Satisfactory data crystals of **1** and **3** were obtained by cutting along cleavage planes, while a suitable specimen of **2**—which fragmented upon attempted cleavage—was acquired by abrading a large crystal in a crystal-tumbling device until it resembled a sphere. The crystals so obtained were glued to glass fibers and examined by precession photography. (Precession photographs of the crystal of **2** were obtained before it was tumbled). After approximate unit cell parameters and probable space groups were determined from precession photographs, each crystal was transferred to an Enraf-Nonius CAD 4 diffractometer controlled by a DEC PDP-8/E computer. Preliminary experiments with the diffractometer confirmed the choices of unit cell and space group and indicated good crystal quality for each specimen. The crystal mosaicities (peak widths at half-peak heights), as determined by  $\omega$  scans with an aperture of 1-mm width, were  $0.18$ – $0.22^\circ$  for intense, low-angle reflections. After accurate centering of 24 high-angle reflections chosen from diverse regions of reciprocal space for the data crystals of **1**, **2**, and **3**, intensity data were gathered as previously reported.<sup>12,13</sup> Crystal data and those variables of data collection that are peculiar to these studies are presented in Table I. The measured intensities were reduced and assigned standard deviations with  $p$  values given in Table I.

Since it was discovered during the solution and refinement of the crystal structure of **3** that the  $\text{Na}^+$  ions are disordered and occupy several different positions, which were assigned partial occupancy parameters, the space group and unit cell were carefully checked. Overexposed precession photographs (24–48 h) of the  $hk0$ ,  $hk1$ ,  $h0l$ ,  $h1l$ , and  $hkk$  zones failed to reveal the presence of a superlattice. Both diffractometer and photographic data showed no evidence of twinning. Hence, we conclude that the disordered model presented herein adequately represents this crystal structure.

Recrystallization of this salt with an equal-volume mixture of water and poly(propylene glycol) yielded crystals that were shown by precession photographs to have the same symmetry and unit cell as that obtained solely from water. Recrystallizations of the  $\text{NH}_4^+$  and  $\text{Mg}^{2+}$  salts of  $[\text{Cu}(\text{EHPG})]^{2-}$  have not been fruitful.

**Solution and Refinement of the Structures.** The structures of **1**–**3** were solved by standard heavy-atom procedures and refined as described earlier.<sup>13</sup> Neutral-atom scattering factors for Ga, Cu, Co, Mg, Na, O, N, C,<sup>14</sup> and H<sup>15</sup> were used in these calculations, with the corrections for anomalous scattering<sup>14</sup> of Mo  $K\alpha$  radiation applied to the atom-scattering curves.

$[\text{Co}(\text{H}_2\text{O})_6][\text{Co}(\text{EHPG})_2] \cdot 4\text{H}_2\text{O}$  (**1**). Full-matrix least-squares refinement of a model structure, in which all non-hydrogen atoms were treated anisotropically, converged with  $R = 0.025$ ,  $R_w = 0.031$ , and the error in an observation of unit weight of  $1.73^{16}$  for 3536

(7) Gaber, B. P.; Miskowski, V.; Spiro, T. G. *J. Am. Chem. Soc.* **1974**, *96*, 6868.

(8) Ainscough, E. W.; Brodie, A. M.; Plowman, J. E.; Brown, K. L.; Addison, A. W.; Gainsford, A. R. *Inorg. Chem.* **1980**, *19*, 3655.

(9) Bailey, N. A.; Cummins, D.; McKenzie, E. D.; Worthington, J. M. *Inorg. Chim. Acta* **1976**, *18*, L13.

(10) Bailey, N. A.; Cummins, D.; McKenzie, E. D.; Worthington, J. M. *Inorg. Chim. Acta* **1981**, *50*, 111.

(11) Sugira, K.; Yamasaki, K. *Nippon Kagaku Zasshi* **1968**, *89*, 853.

(12) Abu-Dari, K.; Raymond, K. N. *Inorg. Chem.* **1980**, *19*, 2034.

(13) The experimental details of data collection and computation involved in the structure analysis are the same as described in: Eigenbrot, C. W., Jr.; Raymond, K. N. *Inorg. Chem.* **1982**, *21*, 2653.

(14) "International Tables for X-Ray Crystallography"; Kynoch Press: Birmingham, England, 1974; Vol. IV.

(15) Stewart, R. F.; Davidson, E. R.; Simpson, W. T. *J. Chem. Phys.* **1965**, *42*, 3175.

(16) The error indices are  $R = \sum |F_o| - |F_c| / \sum |F_o|$  and  $R_w = [\sum w(|F_o| - |F_c|)^2 / \sum w|F_o|^2]^{1/2}$ , and the error in an observation of unit weight =  $[\sum w(|F_o| - |F_c|)^2 / (N_o - N_v)]^{1/2}$ , where  $N_o$  is the number of observations  $|F_o|$  and  $N_v$  is the number of variables.

Table I. Crystallographic Summary<sup>a</sup>

	[Co(H <sub>2</sub> O) <sub>6</sub> ][Co(EHPG)] <sub>2</sub> ·4H <sub>2</sub> O (1)	[Mg(H <sub>2</sub> O) <sub>6</sub> ]- [Ga(EHPG)] <sub>2</sub> ·3H <sub>2</sub> O (2)	Na <sub>2</sub> [Cu(EHPG)]·5.5H <sub>2</sub> O (3)
<i>a</i> , Å	14.818 (2)	20.946 (4)	14.195 (1)
<i>b</i> , Å	16.991 (2)	13.010 (1)	22.607 (3)
<i>c</i> , Å	8.414 (1)	17.002 (3)	14.242 (1)
$\beta$ , deg	91.32 (1)	114.75 (1)	
<i>V</i> , Å <sup>3</sup>	2117.9 (9)	4208 (2)	4570 (1)
<i>d</i> <sub>measd</sub> <sup>b</sup> , g cm <sup>-3</sup>	1.61 (3)	1.56 (3)	1.61 (3)
<i>d</i> <sub>calcd</sub> , g cm <sup>-3</sup>	1.68	1.64	1.64
mol formula	C <sub>36</sub> H <sub>52</sub> Co <sub>3</sub> N <sub>4</sub> O <sub>22</sub>	C <sub>36</sub> H <sub>50</sub> Ga <sub>2</sub> MgN <sub>4</sub> O <sub>21</sub>	C <sub>18</sub> H <sub>27</sub> CuN <sub>2</sub> Na <sub>2</sub> O <sub>11.5</sub>
fw	1069.6	1038.6	564.96
cryst syst	monoclinic	monoclinic	orthorhombic
systematic absences	0 <i>k</i> 0, <i>k</i> = 2 <i>n</i> + 1 0 <i>h</i> l, <i>h</i> + <i>l</i> = 2 <i>n</i> + 1	<i>h</i> 0 <i>l</i> , <i>l</i> = 2 <i>n</i> + 1 <i>hkl</i> , <i>h</i> + <i>k</i> = 2 <i>n</i> + 1	0 <i>kl</i> , <i>k</i> = 2 <i>n</i> + 1 0 <i>h</i> l, <i>l</i> = 2 <i>n</i> + 1 <i>hk</i> 0, <i>h</i> + <i>k</i> = 2 <i>n</i> + 1
space group	<i>P</i> 2 <sub>1</sub> / <i>n</i> (No. 14) <sup>c</sup>	<i>C</i> c (No. 7) or <i>C</i> 2/ <i>c</i> (No. 15) <sup>d</sup>	<i>P</i> <i>b</i> <i>c</i> <i>n</i> (No. 60)
<i>p</i> value	0.02	0.02	0.04
check reflns	random variation in intensity as a function of time for all three data sets; hence no decay corrections necessary.		
2 $\theta$ range, deg	3.0–55.0	3.0–55.0	3.0–55.0
total no. of reflns measd	4667	4814	5236
data cryst dimens, mm	0.15 × 0.23 × 0.29	0.18 × 0.21 × 0.26	0.14 × 0.20 × 0.25
data cryst faces	(110), ( $\bar{1}\bar{1}0$ ), ( $\bar{1}\bar{1}0$ ), ( $\bar{1}10$ ), ( $\bar{1}\bar{1}0$ ), (101), ( $\bar{1}0\bar{1}$ )	<i>e</i>	(210), ( $\bar{2}10$ ), (010), (0 $\bar{1}0$ ), (001), (00 $\bar{1}$ )
abs coeff, $f\mu$ (Mo K $\alpha$ ), cm <sup>-1</sup>	9.36	14.6	13.9

<sup>a</sup> Unit cell parameters were obtained by least-squares refinement of the setting angles of 25 reflections, formed from subgroups of symmetry-related reflections, with  $20.0 < 2\theta < 24.8^\circ$  for 1,  $23.8 < 2\theta < 24.6^\circ$  for 2, and  $14.4 < 2\theta < 28.4^\circ$  for 3. Numbers in parentheses are the estimated standard deviations in the least significant digits. <sup>b</sup> Flotation in a cyclohexane/bromoform mixture. <sup>c</sup> Non standard setting of space group *P*2<sub>1</sub>/*c* with general equivalent positions *x*, *y*, *z*;  $\bar{x}$ ,  $\bar{y}$ ,  $\bar{z}$ ;  $1/2 - x$ ,  $1/2 + y$ ,  $1/2 - z$ ;  $1/2 + x$ ,  $1/2 - y$ ,  $1/2 + z$ . <sup>d</sup> Shown by successful least-squares refinement to be *C*2/*c* (see text). <sup>e</sup> The data crystal was obtained by tumbling a large specimen to an approximate ellipsoid with major and minor axes given in the table. <sup>f</sup> Examination of reflections with  $\chi = 90 \pm 10^\circ$  at approximately regular intervals ( $\Delta(2\theta) \approx 6-10^\circ$ ) within the  $2\theta$  range of data collection by the  $\psi$ -scan technique indicated that all three data crystals had normalized transmission factors within the range 0.95–1.00. Hence absorption corrections were not applied to these data sets.

observations and 295 variables. Hydrogen atoms of the ligand (located from a difference electron density map) were placed and maintained at idealized positions,<sup>17</sup> while those of every water molecule were fixed at positions determined from the difference Fourier map. Hydrogen atoms were assigned isotropic thermal parameters of  $5.0 \text{ \AA}^2$ .

Comparison of  $|F_o|$  and  $|F_c|$  showed no indication of secondary extinction. A structure factor calculation with all 4667 symmetry-independent reflections measured during data collection gave an *R* value of 0.048. In the final cycle of refinement, the largest parameter shift was one-fourth of a corresponding estimated standard deviation (esd). Peaks on the ensuing final difference electron density map were no greater than  $0.3 \text{ e \AA}^{-3}$  and may be compared to heights of  $\sim 3.5 \text{ e \AA}^{-3}$  of water molecule oxygen atoms noted on a previous difference density map. Comparison of  $|F_o|$  vs.  $|F_c|$  showed no trends as a function of  $|F_o|$ ,  $(\sin \theta)/\lambda$ , or Miller index.<sup>18</sup>

[Mg(H<sub>2</sub>O)<sub>6</sub>][Ga(EHPG)]<sub>2</sub>·3H<sub>2</sub>O (2).<sup>19</sup> Full-matrix least-squares convergence was attained for a model structure in which non-hydrogen atoms were refined anisotropically and hydrogen atoms were either placed at idealized positions for those of the EHPG ligand or maintained at positions estimated from a difference Fourier map for those of the water molecules. As above, all hydrogen positions were readily located from a difference Fourier map. In refinement, the hydrogen atoms of EHPG were assigned thermal parameters of  $4.0 \text{ \AA}^2$ , while those of the water molecules were given values of  $5.0 \text{ \AA}^2$ . At convergence, *R* = 0.033, *R*<sub>w</sub> = 0.035, and the error in an observation of unit weight was 1.46 for 3778 observations and 292 variables. From an examination of the data, it was apparent that some of the low-angle

reflections were suffering from secondary extinction. Hence, a small correction<sup>20</sup> [ $3.1 (2) \times 10^{-7} \text{ e}^{-2}$ ] for this effect was applied in the concluding cycles of refinement. A structure factor calculation with all 4814 reflections gathered during data collection gave an *R* index of 0.054. No parameter shift exceeded 0.35 of a corresponding esd in the final cycle of refinement. The largest peaks of a final difference density map were  $\sim 0.2 \text{ e \AA}^{-3}$  (insignificant when compared to the densities of  $5.6-5.7 \text{ e \AA}^{-3}$  of oxygen atoms of water molecules of this structure). Aside from the somewhat unsatisfactory agreement between  $|F_o|$  and  $|F_c|$  for very weak reflections, there were no other anomalies for  $|F_o|$  vs.  $|F_c|$  as a function of  $|F_o|$ ,  $(\sin \theta)/\lambda$ , or Miller index.

Na<sub>2</sub>[Cu(EHPG)]·5.5H<sub>2</sub>O (3). Solution and refinement of the crystal of structure of 3 were not performed as routinely as those of 1 and 2. Although location of the atoms constituting the [Cu(EHPG)]<sup>2+</sup> species—the description of which is the principal objective of this structure analysis—was straightforward, the positions of the Na<sup>+</sup> ions and water molecules of the crystal were far less apparent. It soon became clear that the Na<sup>+</sup> ions occupied positions that, for an average unit cell, could only be partially filled if anomalously short interatomic distances were to be avoided. Hence, numerous difference Fourier syntheses followed by simultaneous least-squares refinement of positional, occupational, and isotropic thermal parameters led to the structure presented herein. All water molecules were ultimately accepted at full occupancy, since their intermolecular distances were within normal limits and their thermal parameters [except perhaps O(12), see below] were also within expected limits. However, it was not possible to fill any of the sites occupied by the Na<sup>+</sup> ions completely because some of these sites fall within 1–2 Å of one another. Site assignment of a Na<sup>+</sup> ion rather than a water molecule was decided primarily by the distances to well-established atoms of the crystal structure and also (but less confidently because of the disorder) by the magnitude of the isotropic thermal parameter. Although the final residuals are low, the resultant refined occupancy parameters for the Na<sup>+</sup> ions [1.74 (3)] yield less positive charge per unit cell than that expected from chemical considerations (i.e., (13.9 (2)) + rather than 16+). We assume the remaining fractional ( $\sim 0.26$ ) Na<sup>+</sup> occupancy lies distributed diffusely elsewhere in the cell, since adjustment of these occupancy parameters prior to refinement to achieve charge balance

(17) The C–H and N–H bonds were constrained to 0.95 and 0.87 Å, respectively, in accordance with a previous study: Churchill, M. R. *Inorg. Chem.* 1973, 12, 1213.

(18) This analysis was made with the Fortran program REVAL, written locally by F. J. Hollander.

(19) The crystal structure of 2 is isostructural with that of [Mg(H<sub>2</sub>O)<sub>6</sub>]-[Fe(EHPG)]<sub>2</sub>·3H<sub>2</sub>O—which was determined in space group *I*2/*c*, an alternate setting of *C*2/*c*. The unit cell parameters reported in ref 10 (*a*<sub>2</sub>, *b*<sub>2</sub>, *c*<sub>2</sub>), are obtained by the transformation of the cell parameters *a*<sub>1</sub>, *b*<sub>1</sub>, *c*<sub>1</sub> selected in our work as

$$\begin{bmatrix} 0 & 0 & 1 \\ 0 & 1 & 0 \\ 1 & 0 & 1 \end{bmatrix} \begin{bmatrix} a_1 \\ b_1 \\ c_1 \end{bmatrix} = \begin{bmatrix} a_2 \\ b_2 \\ c_2 \end{bmatrix}$$

(20) Zachariasen, W. H. *Acta Crystallogr., Sect. A* 1968, A24, 212.

Table II. Fractional Coordinates of the Non-Hydrogen Atoms of  $[\text{Co}(\text{H}_2\text{O})_6][\text{Co}(\text{EHPG})]_2 \cdot 4\text{H}_2\text{O}$  (1)<sup>a</sup>

atom	x	y	z
Co(1)	0.10278 (2)	0.16558 (2)	-0.03831 (3)
Co(2)	0	0	1/2
O(1)	0.14893 (9)	0.08607 (8)	-0.1761 (2)
O(2)	-0.01476 (9)	0.12206 (8)	-0.0810 (2)
O(3)	0.11929 (9)	0.09797 (8)	0.1409 (2)
O(4)	0.08668 (9)	0.23341 (8)	-0.2141 (2)
O(5)	0.22974 (10)	0.03301 (9)	0.2695 (2)
O(6)	-0.01085 (11)	0.32315 (9)	-0.3051 (2)
O(7)	0.07833 (10)	0.10039 (8)	0.5230 (2)
O(8)	-0.04390 (9)	0.03879 (9)	0.2747 (2)
O(9)	0.10312 (10)	-0.06178 (9)	0.3813 (2)
O(10)	0.00302 (11)	0.23917 (10)	0.4076 (2)
O(11)	0.33080 (12)	0.32745 (10)	-0.1121 (2)
N(1)	0.2223 (1)	0.2017 (1)	0.0237 (2)
N(2)	0.0574 (1)	0.2552 (1)	0.0782 (2)
C(1)	0.2032 (1)	0.0826 (1)	0.1741 (2)
C(2)	0.2710 (1)	0.1297 (1)	0.0772 (2)
C(3)	0.3006 (1)	0.0844 (1)	-0.0662 (2)
C(4)	0.3903 (1)	0.0620 (1)	-0.0815 (3)
C(5)	0.4181 (2)	0.0223 (1)	-0.2143 (3)
C(6)	0.3556 (2)	0.0052 (1)	-0.3352 (3)
C(7)	0.2661 (1)	0.0269 (1)	-0.3217 (3)
C(8)	0.2371 (1)	0.0667 (1)	-0.1864 (2)
C(9)	0.2128 (1)	0.2598 (1)	0.1547 (2)
C(10)	0.1340 (2)	0.3101 (1)	0.1100 (3)
C(11)	-0.0140 (1)	0.2879 (1)	-0.0289 (2)
C(12)	-0.0975 (1)	0.2390 (1)	-0.0123 (2)
C(13)	-0.1789 (2)	0.2727 (1)	0.0305 (3)
C(14)	-0.2551 (2)	0.2264 (2)	0.0486 (3)
C(15)	-0.2493 (1)	0.1462 (2)	0.0251 (3)
C(16)	-0.1683 (1)	0.1118 (1)	-0.0158 (2)
C(17)	-0.0909 (1)	0.1574 (1)	-0.0365 (2)
C(18)	0.0221 (1)	0.2831 (1)	-0.1970 (2)

<sup>a</sup> Numbers in parentheses are the estimated standard deviations in the least significant digits. See Figure 5 for identity of the atoms.

(i.e., 16+) dramatically increased the *R* indices and the cation isotropic thermal parameters. Hence the final structure of **3** is that which gave the most satisfactory combination of interatomic contacts, isotropic thermal parameters, and *R* indices. No unusually close  $\text{Na}^+ \cdots \text{Na}^+$  contacts are necessary in this model.

At convergence, for a model in which the non-hydrogen atoms of the  $[\text{Cu}(\text{EHPG})]^{2-}$  complex and the oxygen atoms of the water molecules were refined anisotropically but the disordered  $\text{Na}^+$  ions isotropically, *R*, *R*<sub>w</sub>, and error in an observation of unit weight indices are 0.052, 0.064, and 2.04, respectively, for 2508 reflections and 327 variables (including seven  $\text{Na}^+$  occupancy parameters). Hydrogen atoms of the  $[\text{Cu}(\text{EHPG})]^{2-}$  complex, most of which were located from a difference Fourier map, were included at idealized positions in the closing cycles of refinement with thermal parameters of 5.0 Å<sup>2</sup>. No attempt was made to locate the hydrogen atoms of the water molecules. In the final cycle of refinement, the largest parameter shifts were less than one-tenth of a corresponding esd and the largest peaks on an ensuing final difference map were 0.3–0.6 e Å<sup>-3</sup> and were associated with some of the water molecules. On a previous difference map, the  $\text{Na}^+$  ions appeared as peaks with heights of 1.2–5.5 e Å<sup>-3</sup>. Examination of  $|F_o|$  vs.  $|F_c|$  as a function of  $|F_o|$ ,  $(\sin \theta)/\lambda$ , and Miller index showed the largest discrepancies for the low-angle reflections, as would be expected for a disordered structure.

The thermal parameters of water molecule O(12) are appreciably larger than those of other water molecules in this structure. Since its occupancy parameter refined to a value insignificantly different from 1.0, it was fixed at full occupancy for the concluding cycles of refinement. Its large thermal motion is probably due to disorder about a few closely separated positions, since it coordinates with several disordered  $\text{Na}^+$  ions.

Tables II–IV present atomic positional parameters with corresponding esd's, as derived from the least-squares inverse matrix, for **1–3**. Listings of anisotropic thermal parameters (Tables V–VII), hydrogen atom parameters (Tables VIII–X), and observed and calculated structure factor amplitudes (Tables XI–XIII) are available.<sup>21</sup>

Table III. Fractional Coordinates of the Non-Hydrogen Atoms of  $[\text{Mg}(\text{H}_2\text{O})_6][\text{Ga}(\text{EHPG})]_2 \cdot 3\text{H}_2\text{O}$  (2)<sup>a</sup>

atom	x	y	z
Ga	0.14052 (1)	0.33471 (2)	0.03526 (2)
Mg	0	0.5107 (1)	3/4
O(1)	0.17282 (9)	0.4563 (1)	0.0036 (1)
O(2)	0.04300 (8)	0.3621 (1)	-0.0271 (1)
O(3)	0.13685 (8)	0.3893 (1)	0.1438 (1)
O(4)	0.14818 (8)	0.2618 (1)	-0.0641 (1)
O(5)	0.20706 (9)	0.4494 (2)	0.2745 (1)
O(6)	0.08710 (10)	0.1485 (2)	-0.1644 (1)
O(7)	0	0.3474 (2)	3/4
O(8)	0	0.6703 (2)	3/4
O(9)	0.10571 (9)	0.4959 (2)	0.8244 (1)
O(10)	0.01313 (8)	0.5233 (1)	0.6384 (1)
O(11)	0	0.0114 (2)	1/4
O(12)	-0.01379 (11)	0.1637 (2)	0.3580 (1)
N(1)	0.24173 (9)	0.2991 (2)	0.1246 (1)
N(2)	0.12019 (10)	0.1821 (2)	0.0583 (1)
C(1)	0.1970 (1)	0.4105 (2)	0.2050 (1)
C(2)	0.2602 (1)	0.3885 (2)	0.1835 (1)
C(3)	0.2734 (1)	0.4827 (2)	0.1407 (1)
C(4)	0.3291 (1)	0.5465 (2)	0.1899 (2)
C(5)	0.3451 (1)	0.6331 (2)	0.1522 (2)
C(6)	0.3063 (1)	0.6540 (2)	0.0685 (2)
C(7)	0.2508 (1)	0.5929 (2)	0.0183 (2)
C(8)	0.2310 (1)	0.5083 (2)	0.0538 (1)
C(9)	0.2403 (1)	0.2001 (2)	0.1673 (2)
C(10)	0.1890 (1)	0.1286 (2)	0.1003 (2)
C(11)	0.0745 (1)	0.1458 (2)	-0.0303 (2)
C(12)	0.0014 (1)	0.1870 (2)	-0.0542 (1)
C(13)	-0.0556 (1)	0.1197 (2)	-0.0772 (2)
C(14)	-0.1218 (1)	0.1551 (2)	-0.0940 (2)
C(15)	-0.1321 (1)	0.2595 (2)	-0.0880 (2)
C(16)	-0.0768 (1)	0.3278 (2)	-0.0646 (2)
C(17)	-0.0090 (1)	0.2928 (2)	-0.0479 (1)
C(18)	0.1048 (1)	0.1865 (2)	-0.0923 (2)

<sup>a</sup> Numbers in parentheses are the estimated standard deviations in the least significant digits. See Figure 5 for identity of the atoms.

## Discussion

The crystal structures of **1–3** possess extensive networks of hydrogen bonds. In **1**, the  $[\text{Co}(\text{EHPG})]^-$  ions are hydrogen bonded through ligand oxygen atoms to oxygen atoms of the  $[\text{Co}(\text{H}_2\text{O})_6]^{2+}$  ions and through ligand nitrogen atoms to water molecules of crystallization. In **2**, racemic pairs of  $[\text{Ga}(\text{EHPG})]^-$  ions are related by N(1)–H $\cdots$ O(4) (carboxylate) bonds across crystallographic inversion centers and then further linked via O $\cdots$ H–O bonds to water molecules of  $[\text{Mg}(\text{H}_2\text{O})_6]^{2+}$  ions and to water molecules of crystallization. In **3** the  $[\text{Cu}(\text{EHPG})]^{2-}$  ions are joined at carboxylate atoms O(3) as *C*<sub>2</sub>-related ion pairs by water molecules O(10), which lie along the twofold axes that are parallel to *b* at *z* = ± 1/4; each O(10) molecule is also strongly hydrogen bonded with two O(9) water molecules, each of which, in turn, is bound to a coordinated phenolate atom O(2) of one of the *C*<sub>2</sub>-related  $[\text{Cu}(\text{EHPG})]^{2-}$  complexes. Stereo diagrams of the crystal packing in these salts are available in the supplementary material as Figures 2–4.<sup>21</sup> The atom-numbering scheme used in this paper is given in Figure 5. As in the structures of **1** and **2**, there is additional hydrogen bonding between  $[\text{Cu}(\text{EHPG})]^{2-}$  ions and water molecules coordinated with the  $\text{Na}^+$  ions of the crystal structure. A summary of the hydrogen bonds in these structures is available (Table XIV).<sup>21</sup>

## Description of the Structures and Discussion

**Stereochemical Analysis of Isomers.** While at first glance it may appear that the total number of stereoisomers possible for octahedral complexes of the EHPG ligand is very large, in fact the number of possible isomers is sharply restricted by

(21) Supplementary material; see paragraph at end of paper.

Table IV. Fractional Coordinates of the Non-Hydrogen Atoms of  $\text{Na}_2[\text{Cu}(\text{EHPG})]\cdot 5.5\text{H}_2\text{O}$  (3)<sup>a</sup>

atom	x	y	z	occupational parameter of disordered ions	atom	x	y	z
Cu	0.29688 (5)	0.18077 (3)	0.31492 (6)		N(1)	0.3461 (3)	0.2601 (2)	0.3544 (4)
Na(1)	0.0720 (4)	0.4402 (2)	0.4520 (4)	0.431 (5)	N(2)	0.2688 (4)	0.1678 (2)	0.4508 (4)
Na(2)	0.0340 (6)	0.4558 (3)	0.4127 (6)	0.283 (5)	C(1)	0.2089 (4)	0.2988 (3)	0.2696 (5)
Na(3)	0	0.6188 (3)	1/4	0.183 (3)	C(2)	0.3178 (4)	0.3046 (2)	0.2857 (4)
Na(4)	0.0943 (6)	0.4030 (3)	0.6788 (5)	0.306 (5)	C(3)	0.3686 (4)	0.2967 (3)	0.1944 (5)
Na(5)	-0.006 (2)	0.472 (1)	0.127 (2)	0.151 (5)	C(4)	0.3799 (4)	0.2404 (2)	0.1529 (4)
Na(6)	0.0931 (8)	0.4530 (5)	0.5317 (8)	0.250 (5)	C(5)	0.4241 (4)	0.2383 (3)	0.0642 (4)
Na(7)	0.028 (1)	0.4007 (8)	0.729 (1)	0.136 (5)	C(6)	0.4536 (4)	0.2889 (3)	0.0188 (5)
O(1)	0.3517 (4)	0.1897 (2)	0.1906 (3)		C(7)	0.4429 (5)	0.3431 (3)	0.0609 (4)
O(2)	0.2367 (4)	0.1067 (2)	0.2792 (3)		C(8)	0.4014 (4)	0.3465 (3)	0.1475 (4)
O(3)	0.1725 (3)	0.2497 (2)	0.2819 (4)		C(9)	0.3125 (4)	0.2707 (3)	0.4506 (4)
O(4)	0.4276 (3)	0.1215 (2)	0.3784 (4)		C(10)	0.3192 (5)	0.2148 (3)	0.5050 (5)
O(5)	0.1675 (3)	0.3444 (2)	0.2412 (4)		C(11)	0.2921 (5)	0.1071 (3)	0.4765 (5)
O(6)	0.4280 (4)	0.0462 (2)	0.4769 (4)		C(12)	0.2222 (5)	0.0650 (3)	0.4333 (6)
O(7)	0.1715 (5)	0.4475 (3)	0.3254 (5)		C(13)	0.1813 (5)	0.0221 (3)	0.4904 (6)
O(8)	-0.0011 (4)	0.3558 (3)	0.1332 (4)		C(14)	0.1183 (5)	-0.0187 (3)	0.4538 (6)
O(9)	0.1153 (6)	0.1320 (3)	0.1354 (5)		C(15)	0.0929 (5)	-0.0157 (3)	0.3614 (6)
O(10)	0	0.2092 (5)	1/4		C(16)	0.1324 (5)	0.0275 (3)	0.3051 (5)
O(11)	0.3122 (5)	0.1050 (3)	0.0545 (6)		C(17)	0.1982 (5)	0.0680 (3)	0.3392 (5)
O(12)	0.0946 (8)	0.4780 (5)	0.6938 (6)		C(18)	0.3910 (5)	0.0911 (3)	0.4411 (5)

<sup>a</sup> Numbers in parentheses are the estimated standard deviations in the least significant digits. See Figure 5 for identity of the atoms.

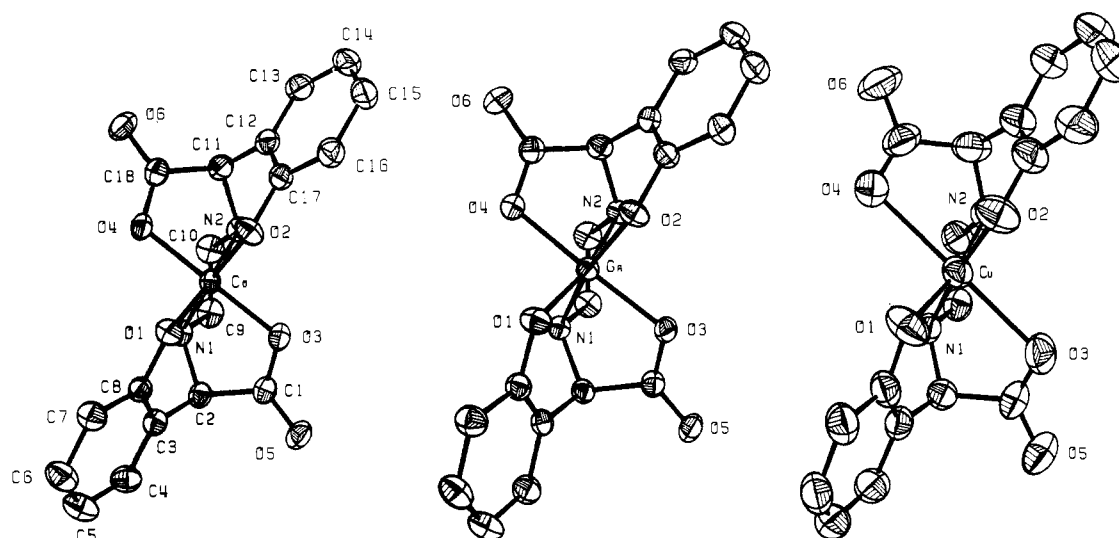


**Figure 5.** Perspective drawings of the EHPG complexes 1–3, as they are viewed down the pseudo-twofold axes of the complexes. The atom-numbering scheme used in this work is shown in full for the Co complex and in part for the Ga and Cu complexes. Atoms are drawn as ellipsoids of 50% probability; hydrogen atoms are not drawn. The configuration about each metal ion is  $\Delta$ -RR, as described in the text. The chiral carbon atom of the upper  $\alpha$ -amino acid unit (C(11)) can be seen to be above the metal ion and nearly on the vertical axis passing through the metal ion. Because the configuration at this carbon atom is *R*, the sequence of ligating groups as viewed counterclockwise down the C–H bond is nitrogen, carboxylate, phenolate. This determines the allowed coordination stereochemistry.

the geometric requirements of the ligand itself. In analysis of the stereoisomers, the formal approach of the IUPAC nomenclature<sup>22</sup> begins with an examination of all of the "skew chelate pairs" that lie along the edges of the pseudooctahedral coordination polyhedron and describe either a left-handed ( $\Lambda$ ) or right handed ( $\Delta$ ) helix. The ordering of these skew chelate pairs, and the subsequent assignment of chirality ( $\Lambda$  or  $\Delta$ ), depends upon the initial reference axis chosen for the molecule. The stereochemistry of EHPG complexes is closely related to that of EDTA (ethylenediaminetetraacetate) and its derivatives.<sup>23</sup> In an earlier description of the stereochemistry of  $\text{Co}(\text{EDTA})^-$ , Legg and Douglas<sup>24</sup> used the molecular  $C_2$  axis as the reference axis. In contrast, we use the reference axis

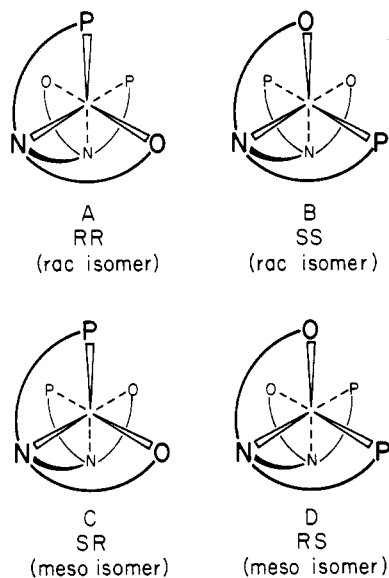
described below for the following reasons: (1) The dominant chirality of the EDTA class of complexes may be viewed as the relationship of the N–N vector to the axis between the two trigonal faces occupied by the two amino acid groups of the ligand. (2) The chiralities of the  $\alpha$ -amino acid groups at either end of the EHPG ligand determine the ordering of the ligating atoms of these trigonal faces and hence define the possible isomers.

The nitrogen, carboxylate, and phenolate ligating groups of one end of the EHPG ligand are constrained by geometry to mutually cis positions, so that they define one face of the octahedral complex. The opposite face is thus occupied by the same ligating atoms from the other end of the EHPG ligand. The axis normal to these faces is chosen as the reference axis and is the view direction of the following coordination diagram. Since the nitrogens are also constrained to be cis to each other, the stereochemistry of the complex is totally specified by the chirality at the metal center ( $\Lambda$  for each of structures A–D) and the sequence in which the ligating

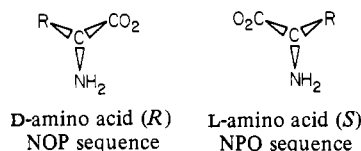
(22) The symbolism for the absolute configurations of six-coordinate complexes based on the octahedron and for the conformation of five-membered chelate rings is given in: *Inorg. Chem.* **1970**, *9*, 1.

(23) Legg, J. I.; Neal, J. A. *Inorg. Chem.* **1973**, *12*, 1805.

(24) Legg, J. I.; Douglas, B. E. *J. Am. Chem. Soc.* **1966**, *88*, 2697.



atoms of the top and bottom faces appear. If O and P represent the ligating oxygen atoms of the carboxylate and phenolate groups, respectively, and the sequence is specified in a right-handed (counterclockwise) sense around the reference axis as viewed down that axis, this sequence can only be NPO or NOP. For the chiral carbon atom of the  $\alpha$ -amino acid group that ligates the top face of structures A–D, the chirality of the amino acid determines the sequence of the ligating groups:



For the racemic EHPG ligand with the *RR* configuration, carbon chirality then specifies only the sequence NOP (top face), NPO (bottom face—in which the C–H vector points down relative to the view direction shown in the sketch). For a  $\Delta$  configuration at the metal, this defines one isomer with structure A. In fact this  $\Delta RR$  structure (and its mirror image  $\Delta SS$ ) is that observed in all of the racemic complexes studied to date and is the structure of each of the complexes shown in Figure 5. The combination of  $\Delta$  metal chirality and the *RR* ligand results in an isomer whose structure is the mirror image of structure B and that molecular models show to be possible but strained. Notice that for *RR* or *SS* ligand both structures A and B have  $C_2$  symmetry (see Table XV) while for *RS* or *SR* ligand structures C and D are equivalent (related by  $C_2$  symmetry).

For the meso form of the ligand (*RS*) with the *R* configuration placed on the top face, the sequence NOP (top), NPO (bottom) specifies structure C. The  $\Delta$  form of the *RS* ligand complex gives the mirror-image isomer.

In summary, for both the racemic and meso forms of the EHPG ligand there is only one stable isomer (each optically active). For the *RR* ligand this isomer is  $\Delta RR$  with structure A (the configuration in Figure 5); a less stable isomer, which has not been observed, is  $\Delta RR$  (the mirror image of structure B). The mirror image of the *SS* ligand forms the corresponding mirror image structures [i.e., the  $\Delta SS$  form (mirror image of structure A) is the stable isomer]. Finally, the meso form of the ligand forms the racemic pair  $\Delta RS$  and  $\Delta RS$  with structure C.

Because of the gauche conformation of the ethylenediamine portion of the EHPG ligand when viewed down the C–C bond (see Table XVI), there are two orientations possible for the

C–C vector with respect to the N–N vector. These conformations ( $\delta$  or  $\lambda$ ) have been analyzed in detail for many ethylenediamine complexes.<sup>25–27</sup> The structures diagrammed in Figure 5 (with our definition of the chirality at the metal center and the IUPAC<sup>22</sup> definition of the conformation helicity) are all  $\Delta\delta$ .

$[\text{Co}(\text{H}_2\text{O})_6][\text{Co}(\text{EHPG})_2] \cdot 4\text{H}_2\text{O}$  (1) and  $[\text{Mg}(\text{H}_2\text{O})_6][\text{Ga}(\text{EHPG})_2] \cdot 3\text{H}_2\text{O}$  (2). Selected bond lengths and angles for the three  $[\text{M}(\text{EHPG})]^{n-}$  complexes of 1–3 ( $n = 1$  or 2) are given in Table XVII. Examination of these values readily shows the expected similarities between the  $[\text{Co}(\text{EHPG})]^-$  and  $[\text{Ga}(\text{EHPG})]^-$  coordination geometries, similarities that are also found in the structures of the  $[\text{Fe}(\text{EHPG})]^-$  complexes.<sup>9,10</sup> The variations in the cis bond angles at the coordinated metal ions of these EHPG complexes of 83–97° in 1 and 79–97° in 2 reflect a consequence of the strain resulting from the coordination of this hexadentate ligand.

The  $[\text{Co}(\text{H}_2\text{O})_6]^{2+}$  ions of 1 occupy sites of  $C_1$  symmetry with Co(II)–O bond lengths that average 2.10 (2) Å, in agreement with the distances determined in two other crystal structures [2.08 (2)<sup>28</sup> and 2.079 (6) Å<sup>29</sup>]. The cis O–Co–O angles are within 4° of the octahedral value of 90°.

The  $[\text{Mg}(\text{H}_2\text{O})_6]^{2+}$  ions of 2 reside at sites of  $C_2$  symmetry, with  $\text{Mg}^{2+}$  and water molecules O(7) and O(8) lying along crystallographic  $C_2$  axes. The Mg–O distances (Table XVI–II<sup>21</sup>), like those of  $[\text{Co}(\text{H}_2\text{O})_6]^{2+}$  in 1, vary significantly; the angles about  $\text{Mg}^{2+}$  deviate by less than 6° from ideal values.

$\text{Na}_2[\text{Cu}(\text{EHPG})] \cdot 5.5\text{H}_2\text{O}$  (3). The most interesting structural features of this series of complexes are exhibited by the  $[\text{Cu}(\text{EHPG})]^{2-}$  species and are consistent with the usual tetragonal distortion seen in six-coordinate complexes of Cu(II).<sup>30</sup> Thus, whereas the M–O bond lengths in the Fe, Co, and Ga complexes vary by only  $\sim 0.1$  Å, the *trans*-M–O(carboxylate) bonds in  $[\text{Cu}(\text{EHPG})]^{2-}$  are 0.4–0.5 Å longer than the M–O(phenolate) bonds. Furthermore, scrutiny of Table XVII reveals that, while the geometries of the carboxylate moieties of the Co and Ga (and also Fe<sup>9,10</sup>) complexes are consistent with anticipated structural features [i.e., C–O (coordinated) bonds are slightly longer than C–O (uncoordinated) bonds and C–C–O (coordinated) angles are smaller than C–C–O (uncoordinated) angles<sup>30</sup>], contradictory results are found in 3. This is probably due to the interaction of the carboxylate oxygen atoms with the  $\text{Na}^+$  ions as well as with the  $\text{Cu}^{2+}$  ions in 3, an effect not found in 1 and 2. Another anomaly is the long C(1)–C(2) bond [1.568 (5) Å], which is formed with one of the carboxylate atom and which may be an artifact of the structure.

As a result of distributional disorder, the coordination environments of the  $\text{Na}^+$  ions of this structure appear somewhat irregular and perhaps are not fully determined. That is, it may be that additional water molecules of partial occupancy (bound to  $\text{Na}^+$  ions) have not been located. Although the range of Na–O distances of 1.70–2.80 Å is broad and a few of the distances appear to be short, most of these values (see Table

- (25) Raymond, K. N.; Corfield, P. W. R.; Ibers, J. A. *Inorg. Chem.* **1968**, *7*, 842.  
 (26) Gollgoly, J. R.; Hawkins, C. J. *Inorg. Chem.* **1969**, *8*, 1168.  
 (27) Smolenaers, P. J.; Beattie, J. K.; Hutchinson, N. D. *Inorg. Chem.* **1981**, *20*, 2202.  
 (28) Nassinbeni, L. R.; Percy, G. C.; Rodgers, A. L. *Acta Crystallogr., Sect. B* **1976**, *B32*, 1252.  
 (29) Lynton, H.; Siew, P.-Y. *Can. J. Chem.* **1973**, *51*, 227.  
 (30) Couldwell, C.; Prout, K.; Robey, D.; Taylor, R.; Rossoti, F. J. C. *Acta Crystallogr., Sect. B* **1978**, *B34*, 1491.  
 (31) The observed trends in the bond distances and angles for the Fe,<sup>10</sup> Co, and Ga complexes parallel data reported for hydrogen-bonded carboxylic acid dimers: Donohue, J. *Acta Crystallogr., Sect. B* **1968**, *B24*, 1558.  
 (32) A difference Fourier map computed only with reflections with  $(\sin \theta)/\lambda < 0.24$  revealed no additional peaks that behaved satisfactorily in least-squares refinement.

Table XV. Deviations of Pseudosymmetrically Related Atoms from  $C_2$  Symmetry

atom 1	atom 1' <sup>b</sup>	dev, <sup>a</sup> Å			
		[Co(EHPG)] <sup>-</sup>	[Ga(EHPG)] <sup>-</sup>	[Cu(EHPG)] <sup>2-</sup>	[Fe(EHPG)] <sup>-c</sup>
M	M	0.031	0.093	0.089	0.096
O(1)	O(2)	0.090	0.316	0.228	0.323
O(3)	O(4)	0.043	0.294	0.124	0.309
N(1)	N(2)	0.032	0.120	0.047	0.125
O(5)	O(6)	0.092	0.337	0.193	0.362
C(1)	C(18)	0.032	0.120	0.048	0.126
C(2)	C(11)	0.020	0.096	0.037	0.099
C(3)	C(12)	0.017	0.081	0.044	0.076
C(4)	C(13)	0.046	0.199	0.039	0.208
C(5)	C(14)	0.054	0.301	0.103	0.319
C(6)	C(15)	0.015	0.102	0.194	0.103
C(7)	C(16)	0.030	0.125	0.038	0.132
C(8)	C(17)	0.039	0.170	0.094	0.179
C(9)	C(10)	0.057	0.165	0.103	0.170
mean dev <sup>d</sup>		0.043	0.180	0.091	0.188
rms dev <sup>e</sup>		0.049	0.201	0.108	0.211

<sup>a</sup> Deviations were obtained by an iterative procedure using the Fortran program BMFIT (Liu, L.-K. Ph.D. Dissertation, University of Texas, Austin, TX, 1977) and are presented as absolute values. <sup>b</sup> See Figure 5 for the identity of the atoms. "M" represents the appropriate complexed metal ion. Atom 1' is the atom related by pseudo- $C_2$ -symmetry to atom 1. <sup>c</sup> These values were obtained from the atomic coordinates reported for the  $Mg^{2+}$  salt in ref 10. <sup>d</sup> A mean deviation is given by  $\sum_i \Delta d_i / n$ , where  $\Delta d_i$  is the minimized distance between atom 1 and atom 1' and  $n$  is the number of pseudosymmetrically related atom pairs. <sup>e</sup> The rms deviation is obtained from  $[\sum_i (\Delta d_i)^2 / n]^{1/2}$ .

Table XVI. Assessment of the Conformation of the Metal Ethylenediamine Rings<sup>a</sup>

	[Co(EHPG)] <sup>-</sup>	[Ga(EHPG)] <sup>-</sup>	[Cu(EHPG)] <sup>2-</sup>
Deviations (Å) of Ethylene Atoms from the M/N(1)/N(2) Planes <sup>b</sup>			
C(9)	-0.372 (2)	-0.290 (3)	0.348 (6)
C(10)	0.356 (2)	0.412 (3)	-0.340 (7)
Torsion Angles (deg) about the Bonds of the C-N-M-N-C Rings <sup>c</sup>			
M-N(1)	-15.2	-11.9	-14.4
N(1)-C(9)	41.8	38.3	40.3
C(9)-C(10)	-54.0	-54.2	-53.3
C(10)-N(2)	41.1	42.3	39.3
N(2)-M	-14.6	-16.9	-14.0
Crossing Angle (deg) between the C-C Bond and N-N Axis <sup>d</sup>			
$\alpha$	29.3	27.6	27.6

<sup>a</sup> See Figure 5 for identity of the atoms. <sup>b</sup> Numbers in parentheses are the estimated standard deviations in the least significant digit. <sup>c</sup> "M" represents Co, Ga, or Cu. The chirality for all of the complexes as tabulated here are the same as shown in Figure 5. <sup>d</sup> The crossing angle ( $\alpha$ ) is defined in ref 25.

XVIII<sup>21</sup>) fall within the bounds of distances (2.2–2.7 Å) commonly observed in ordered structures. Moreover, the coordination spheres (some of which may not be fully characterized) of these  $Na^+$  ions approximate expected polyhedra, namely octahedral [Na(3) and Na(4)], square pyramidal [Na(1), Na(2), and Na(5)], trigonal bipyramidal [Na(7)], and tetrahedral [Na(6)]. It is noteworthy that the  $Na^+$  ions of the [Fe(EHPG)]<sup>-</sup> crystal structure are also disordered over several sites, although there charge balance was achieved.<sup>9,10</sup> Such disorder is apparently a manifestation of the multitude of satisfactory  $Na^+$  coordination environments offered by the oxygen atoms of the water molecules and the complexed EHPG ligands in these crystal structures (as may be seen in the packing diagrams<sup>21</sup>).

**Relevance of Structures 1–3 to Transferrin.** Considerable effort has been expended in determining the types and number of chelating groups in the transferrin active site. There are probably two nitrogen atoms from histidine residues,<sup>33</sup> two phenolic oxygen atoms from tyrosine moieties,<sup>34,35</sup> a (bi)-

carbonate ion,<sup>36,37</sup> and a water molecule<sup>38</sup> or hydroxide ion<sup>4,5</sup> bound to the ferric ion. The structures presented herein and elsewhere<sup>9,10</sup> indicate that the hexadentate EHPG ligand offers an octahedral coordination environment to metal ions that consists of the same number and types of heteroatoms as are found in the transferrin binding sites.

Often a small molecule model may give information about the metal binding site of a protein. Metal-EHPG complexes have been shown to model accurately many of the physical properties of not only diferric transferrin but other  $M_2$ -transferrin complexes as well.<sup>4–8,39</sup> In addition, the different isomers of EHPG may be used to determine the disposition of metal binding moieties at the active site. However, before such insight may be gained, a detailed knowledge of the solid state and solution chemistry of the model must be gathered.

The most striking difference between the meso and racemic isomers is the coordination geometry about the metal ion. Complexation of the metal ion by the racemic isomer (as described in the section on stereochemical analysis of the isomers) occurs via trans carboxylate coordination, whereas in the meso species all ligating groups are cis. This difference has a significant impact on the stability of the metal complexes of the two isomers. Bernauer<sup>40</sup> has reported that the ferric complex of the meso isomer is 1.65 kcal/mol less stable than the corresponding racemic complex ( $\log K_{ML}(\text{meso}) = 33.8$ ,  $\log K_{ML}(\text{rac}) = 35.0$ ). He suggests that this difference in stability is due to the coordination of one five-membered ring and two six-membered rings in the same plane in the trans carboxylate complex (structure A as shown in the earlier schematic diagram) as contrasted to the arrangement in the meso complex (structure C) in which two five-membered rings and one six-membered ring bond to the metal in the same plane. Since the bite angle of a six-membered ring ( $\approx 90$ – $95^\circ$ ) is substantially greater than that of a five-membered ring ( $\approx 75$ – $80^\circ$ ), more satisfactory octahedral coordination is achieved with both six-membered rings bound to the metal

(33) Rogers, T. B.; Gold, R. A.; Feeney, R. E. *Biochemistry* **1977**, *16*, 2299.  
 (34) Tan, A. T.; Woodworth, R. C. *Biochemistry* **1969**, *8*, 3771.  
 (35) Geoghegan, K. F.; Callas, J. L.; Feeney, R. E. *J. Biol. Chem.* **1980**, *255*, 11429.

(36) Bates, G. W.; Schlabach, M. R. "Proteins of Iron Storage and Metabolism in Biochemistry and Medicine"; Crichton, R. R., Ed.; North-Holland Publishing Co.: Amsterdam, 1975; p 51.  
 (37) Gelb, M. H.; Harris, D. C. *Arch. Biochem. Biophys.* **1980**, *200*, 93.  
 (38) Koenig, S. H.; Schillinger, W. E. *J. Biol. Chem.* **1969**, *244*, 6520.  
 (39) Prados, R.; Boggess, R. K.; Martin, R. B.; Woodworth, R. C. *Bioinorg. Chem.* **1975**, *4*, 135.  
 (40) Bernauer, K. *Top. Curr. Chem.* **1976**, *65*, 1.

Table XVII. Bond Lengths (Å) and Bond Angles (deg)<sup>a</sup>

	[Co(EHPG)] <sup>-</sup>	[Ga(EHPG)] <sup>-</sup>	[Cu(EHPG)] <sup>2-</sup>
M-O(1) <sup>b</sup>	1.917 (1)	1.886 (2)	1.944 (3)
M-O(2)	1.918 (1)	1.899 (1)	1.937 (3)
M-O(3)	1.907 (1)	2.009 (2)	2.404 (3)
M-O(4)	1.886 (1)	2.002 (2)	2.462 (3)
M-N(1)	1.935 (1)	2.078 (2)	2.010 (3)
M-N(2)	1.940 (1)	2.102 (2)	1.999 (3)
O(1)-C(8)	1.353 (2)	1.344 (3)	1.326 (4)
O(2)-C(17)	1.339 (2)	1.345 (3)	1.337 (5)
O(3)-C(1)	1.295 (2)	1.284 (3)	1.239 (5)
O(4)-C(18)	1.286 (2)	1.285 (3)	1.239 (5)
O(5)-C(1)	1.222 (2)	1.221 (3)	1.250 (5)
O(6)-C(18)	1.228 (2)	1.224 (3)	1.254 (5)
N(1)-C(2)	1.485 (2)	1.477 (3)	1.458 (5)
N(1)-C(9)	1.488 (2)	1.483 (3)	1.473 (5)
N(2)-C(10)	1.488 (2)	1.487 (3)	1.484 (5)
N(2)-C(11)	1.482 (2)	1.487 (3)	1.466 (5)
C(1)-C(2)	1.533 (2)	1.540 (3)	1.568 (5)
C(2)-C(3)	1.505 (2)	1.510 (3)	1.503 (5)
C(9)-C(10)	1.489 (2)	1.513 (3)	1.505 (5)
C(11)-C(12)	1.501 (2)	1.510 (3)	1.499 (6)
C(11)-C(18)	1.525 (2)	1.538 (3)	1.537 (7)
mean phenyl C-C <sup>c</sup>	1.390 (3)	1.388 (4)	1.387 (6)
M-O(1)-C(8)	124.7 (1)	125.4 (1)	125.4 (2)
M-O(2)-C(17)	122.8 (1)	125.8 (1)	124.7 (3)
M-O(3)-C(1)	113.4 (1)	114.7 (1)	107.5 (2)
M-O(4)-C(18)	113.2 (1)	112.5 (1)	104.5 (3)
M-N(1)-C(2)	104.8 (1)	102.6 (1)	109.2 (2)
M-N(1)-C(9)	108.0 (1)	109.1 (1)	107.3 (2)
C(2)-N(1)-C(9)	112.1 (1)	113.4 (2)	114.6 (3)
M-N(2)-C(10)	108.2 (1)	107.5 (1)	107.7 (2)
M-N(2)-C(11)	103.8 (1)	102.0 (1)	109.3 (2)
C(10)-N(2)-C(11)	113.9 (1)	114.5 (2)	114.9 (3)
O(3)-C(1)-O(5)	125.0 (2)	125.8 (2)	126.0 (4)
O(3)-C(1)-C(2)	114.6 (1)	114.7 (2)	117.7 (4)
O(5)-C(1)-C(2)	120.3 (1)	119.4 (2)	116.2 (4)
C(1)-C(2)-C(3)	111.5 (1)	108.1 (2)	109.5 (3)
C(1)-C(2)-N(1)	105.8 (1)	107.9 (2)	108.7 (3)
C(3)-C(2)-N(1)	109.1 (1)	111.0 (2)	111.5 (3)
C(2)-C(3)-C(4)	120.7 (1)	118.3 (2)	119.0 (4)
C(2)-C(3)-C(8)	119.1 (1)	122.4 (2)	121.4 (3)
O(1)-C(8)-C(3)	122.4 (1)	123.6 (2)	125.1 (4)
N(1)-C(9)-C(10)	106.3 (1)	108.6 (2)	108.2 (3)
C(9)-C(10)-N(2)	106.0 (1)	108.3 (2)	107.6 (3)
N(2)-C(11)-C(12)	108.3 (1)	107.9 (2)	109.9 (4)
N(2)-C(11)-C(18)	106.4 (1)	108.6 (2)	110.3 (3)
C(12)-C(11)-C(18)	111.4 (1)	110.8 (2)	108.7 (4)
C(11)-C(12)-C(13)	121.3 (2)	120.4 (2)	118.7 (5)
C(11)-C(12)-C(17)	118.2 (1)	120.0 (2)	121.5 (4)
O(2)-C(17)-C(1)	123.1 (1)	123.0 (2)	123.8 (4)
C(11)-C(18)-O(4)	114.6 (1)	115.8 (2)	119.3 (4)
C(11)-C(18)-O(6)	121.0 (2)	120.7 (2)	116.3 (4)
O(4)-C(18)-O(6)	124.4 (2)	123.5 (2)	124.4 (5)

<sup>a</sup> Numbers in parentheses are the estimated standard deviations in the least significant digits. See Figure 5 for identity of the atoms. <sup>b</sup> "M" represents the appropriate metal ion bound to the EHPG ligand. <sup>c</sup> A mean bond length is given by  $\bar{l} = \sum_i l_i/n$  and its standard deviation by  $[\sum(l_i - \bar{l})^2/n(n-1)]^{1/2}$ , where  $n$  is the number of equivalent bonds.

in the plane that contains the five-membered ethylenediamine group.

As noted earlier, for the racemic ligand isomer with a  $\Delta$  configuration about the metal, only structure A is stable and that is the geometry observed (Figure 5). The *meso*-[Fe(EHPG)]<sup>-</sup> complex,<sup>9,10</sup> as the  $\Delta$  isomer, has only been observed as isomer C, with a  $\delta$  ethylenediamine ring conformation.

Thus, the stable isomers and conformations of the complexes observed to date follow the predictions of the stereochemical analysis presented earlier in this paper.

Martell et al.<sup>41</sup> have reported the solution equilibria of an unspecified mixture of EHPG with Cu(II). They proposed that in basic solution EHPG acts as a tetradentate ligand using the ethylenediamine nitrogen and the phenolic oxygen atoms to form a square-planar complex and that the carboxylate groups are not bound to the metal. Examination of 3 demonstrates that, at least in the solid state, the  $\Delta RR\delta$  ( $\Delta SS\lambda$ ) isomers of EHPG bind as a hexadentate chelating agent with the carboxylate oxygens weakly coordinating in axial positions. Because of the large tetragonal distortion, the differences in stability between the *rac*- and *meso*-[Cu(EHPG)]<sup>2-</sup> isomers should be greater than that between the corresponding [Fe(EHPG)]<sup>-</sup> complexes. That is, coordination of Cu(II) by *meso*-EHPG would require that a phenolate group occupy an elongated axial position, thereby imparting additional instability to the complex.

The difference in stability of the  $\Delta RR\delta$  ( $\Delta SS\lambda$ ) and  $\Delta RS\delta$  (racemic and *meso*) complexes may produce a change in the visible spectrum. The presumably inequivalent interaction between the phenolate moieties and Cu(II) in the two complexes would suggest that the charge-transfer characteristics of the racemic and *meso* chelates would be altered, since the origin of the 375-nm transition in these complexes is exclusively metal-phenolate in character.<sup>7,39</sup> Indeed,  $\lambda_{\max}$  for a mixture of [Cu(EHPG)]<sup>2-</sup> isomers is observed at 375 nm (pH > 6),<sup>41</sup> whereas a band at 381 nm is found for the pure<sup>42</sup> *meso*-[Cu(EHPG)]<sup>2-</sup>.

Spiro et al.<sup>7</sup> have reported previously that [Cu(EHPG)]<sup>2-</sup> does not show an intense charge-transfer band as is observed in Cu<sub>2</sub>(transferrin) and thus proposed that EHPG binding of Cu(II) is via equatorial coordination of amine and carboxylate groups, with weak axial phenolic interactions (structure B). This is contradicted by the structure reported here. No phenolate charge-transfer band was observed in the previous study<sup>7</sup> because the experiments were carried out at pH 8, and at this pH the [Cu(EHPG)]<sup>2-</sup> complex is not fully formed.<sup>41</sup> Only at slightly higher pH does the complex fully form and the phenolate charge-transfer band develop.

**Acknowledgment.** We thank Professor N. A. Bailey for a preprint describing the crystal structures of the [Fe(EHPG)]<sup>-</sup> complexes and Dr. F. J. Hollander of the CHEXRAY Crystallographic Facility University of California, Berkeley, CA, for useful discussions. This work was supported by NIH Grant No. HL 24775.

**Registry No.** 1, 86852-04-2; 2, 86823-52-1; 3, 86852-60-0.

**Supplementary Material Available:** Listings of anisotropic thermal parameters (Tables V-VII), fractional coordinates and assigned isotropic thermal parameters (Tables VIII-X), observed and calculated structure factor amplitudes (Tables XI-XIII), selected nonbonded distances (Table XIV), and cation bond lengths (Table XVIII) and stereoscopic views of the anions (Figures 2-4) (75 pages). Ordering information is given on any current masthead page.

- (41) Frost, A. E.; Freedman, H. H.; Westerback, S. J.; Martell, A. E. *J. Am. Chem. Soc.* **1958**, *80*, 530.  
 (42) Details for the purification of the *meso* isomer are given in: Patch, M. G.; Simolo, K. S.; Carrano, C. J. *Inorg. Chem.* **1983**, *22*, 2630.